Catalysis Science & Technology

Accepted Manuscript

ROYAL SOCIETY OF CHEMISTRY

www.rsc.org/catalysis

Superior performance of mesoporous tin oxide over nano and bulk in activation of carbonyl group: Conversion of bio-renewable feedstock

Vijaykumar S. Marakatti, Pandian Manjunathan, Anand B. Halgeri and Ganapati V. Shanbhag*

[a] *Materials Science Division, Poornaprajna Institute of Scientific Research (PPISR),Bidalur Post, Devanahalli, Bangalore-562110, India.*

(*Corresponding authors: shanbhag@poornaprajna.org, Tel: +9180-27408552, Fax: +9180-23619034)

Abstract:

The efficiency of mesoporous tin oxide as an acid catalyst in activation of carbonyl group through selected organic transformations involving the conversion of biomass derived molecules to value-added chemicals is reported. The mesoporous tin oxide was synthesized at ambient temperature using CTAB and characterized by XRD, FT-IR, SEM, TEM,TGA, N_2 Sorption, TPD-NH_3 and py-FT-IR. The mesoporous tin oxide calcined at different temperatures showed different physico-chemical properties. The mesoporous tin oxide exhibited wormhole like topology with large surface area of 160 m^2/g. The py-FT-IR acidity measurement of mesoporous tin oxide showed the presence of Brönsted and Lewis acid sites. These acid sites were sufficient to activate the carbonyl groups of aldehyde, ketone, acetic anhydride and amide in selected important organic transformations such as Prins condensation, glycerol carbonylation with urea, ketalization of glycerol with cyclohexanone and acetylation of glycerol with acetic anhydride. In all the above catalytic processes, mesoporous tin oxide showed superior performance compared to nano and bulk tin oxide. Mesoporous tin oxide catalyst also showed excellent recyclability and remarkable activity compared to reported catalyst in all the reactions under study.

Keywords: Mesoporous; Tin oxide; Carbonyl group; Glycerol; β-pinene: Nopol

1. Introduction

After the discovery of MCM-41 and M41S family of materials, mesoporous materials have received much attention because of their diverse composition, pore system, large surface area and novel properties.[1,2] As a consequence, mesostructured materials have been widely applied in the field of catalysis, molecular sieves, gas sensors and solid state ionic devices. Initially, siliceous mesostructured materials (MCM-41, MCM-48, SBA-15, KIT-6) have been synthesized by supra molecular templating approach which was further extended for the synthesis transition and main group metal oxides.[3-6] Mesoporous oxides of W, Sb and Pb were first reported and subsequently other mesostructured oxides of Al, Ti, Nb and Zr were synthesized by different templating routes.[7-11] However, these mesoporous metal oxide materials suffer from disadvantages such as semicrystalline pore walls, low crystallinity and thermal stability. Nevertheless, these materials have been used in several noteworthy applications and have exhibited excellent performances.[12]

The advantage of metal oxide as a catalyst lies in its simple preparation step (easy industrial scale up), high thermal-mechanical stability and no leaching of active sites during the reaction (as leaching is observed in supported catalyst). Traditionally, bulk metal oxides have been widely investigated for the energy conversion and storage, catalysis, sensing, adsorption and separation.[13] The presence of low surface area, absence of porosity and large particle size had an enormous difficulty on such applications. However, the nano materials with high surface area and small particle size boomed over bulk materials. Nevertheless, synthesis of uniform particle size, separation of catalyst and agglomerization of particles are the difficulties associated with nano materials. Due to high surface area and large pore size mesostructured materials exhibits different physical and chemical properties over nano and bulk materials which in turn

makes valuable application in several fields. Therefore, the mesoporous materials with considerably large amount of active sites and porosity (easy diffusion of reactants) could significantly exhibit higher performance. The mesoporous $Li_{1.12}Mn_{1.88}O_{44}$ showed remarkable activity in Li-ion battery application compared to nano and bulk phase.[14] The single crystalline mesoporous tin oxide showed higher catalytic activity than the commercial P-25 and polycrystalline TiO_2 in cinnamyl alcohol oxidation to cinnamaldehyde. [15] The mesoporous tin oxide showed high cycle life performance and rate capabilities than the nano tin oxide.[16] These results stimulated us to study the application of different forms of tin oxide as an acid catalysts for important organic reactions. Therefore, the catalytic application of mesoporous tin oxide and its advantages over nano and bulk tin oxide materials were studied for the transformation of bio-mass derived molecules.

Tin oxide was mainly studied as n-type semiconductor material with wide band gap used basically in gas sensor, as an electrode material in Li-ion batteries and other optical electronic devices.[17, 18] Moreover, tin oxide was applied as catalyst and catalyst support in several oxidation and hydrogenation reactions.[19,20] However, there are no reports on the application of bare mesoporous tin oxide as an acid catalyst. The acidity of metal oxide mainly depends on the percentage ionic character of metal-oxygen bond and oxidation state of metal. The metal oxide with low percentage ionic character and high oxidation state possesses more acidity. Among the different metal oxides, Sn with lower percentage ionic character (42.2) and higher oxidation state of +4 could show high acidity which can catalyze certain reaction.[21] Moreover, the nature and amount of acidic sites, physical properties (surface area, pore volume) influence on activation of reactant molecules in several organic transformation.

The utilization of biomass, in particular biodiesel synthesis, has received much attention in the last decades. Its budding application as an alternative to fossil fuels establishes a green alternative route to reduce carbon emissions.[22, 23] One of the major difficulties of the biodiesel industry is the production of large amounts of glycerol as a byproduct by trans-esterification of fatty acids. Therefore, conversion of glycerol to value added chemicals is desirable and has become a broad area of research. In recent years, chemical transformation of glycerol into more economical valuable products has attracted the attention of scientific community. In this regard considerable research interest has been done to synthesized glycerol derivatives such as acrolein, propylene glycol, 1,3-propanediol, glyceric acid, glycerol carbonate, solketal and ethers etc, which find their wide application in soap-detergent, battery, perfumery and polymer industries.[24-26] β-pinene is another inexpensive and worldwide available class of biomolecule derived from pine tree. The effective conversion of this pinene to value-added chemicals is an important area of research.[27] The bio-oil obtained from fast pyrolysis contains a range of carboxylic acids, aldehydes, and ketones.[28] Therefore conversions of these highly oxygenates molecules require the use of catalysts that can selectively activate their carbonyl group to promote desired reaction pathways, such as C-C bond-forming condensations and isomerization reactions.[28] Considering the above facts, four important organic transformations were selected for the study concerning conversion of bio-mass derived molecules *viz.* β-pinene to nopol, glycerol acetylation to acetins, carbonylation of glycerol to glycerol carbonate and kealization of glycerol to cyclic ketal which proceed through activation of carbonyl group.

We recently reported metal ion-exchanged zeolites as active catalysts for the conversion of bio-renewable feedstock.[29-31] In continuation of our investigation on simple, efficient and environmentally friendly catalysts for the conversion of biomass derived molecules, herein, we

report the applications of mesoporous tin oxide as solid acid catalyst for the conversion of bio-renewable feedstock to value-added chemicals. The NiSb/SBA-15 was synthesized by at room temperature and characterized by XRD, SEM, TEM, FT-IR, N_2 Sorption, TPD-NH_3 and py-FTIR. Four important organic transformations were selected involving conversion of bio-mass derived molecules *viz.* Prins condensation of β-pinene to nopol, glycerol acetylation to acetins, carbonylation of glycerol to glycerol carbonate and kealization of glycerol to cyclic ketal which proceed through activation of carbonyl group. The catalytic performance of mesoporous tin oxide was related with bulk and nano tin oxide. The amount of acidity and the nature of acidic sites i.e. Brönsted and Lewis acid sites of mesoporous tin oxide were correlated with catalytic activity in all the organic reactions. The catalyst recyclability and their comparison with other reported catalysts were also investigated.

2. Experimental section

2.1. Synthesis of catalyst

The mesostructured tin oxide was synthesized at room temperature using $SnCl_4.5H_2O$ and cetyltrimethylammonium bromide (CTAB) as template.[32,33] In a typical procedure, 18 g of CTAB was dissolved in 150 ml of water under stirring to get a homogeneous solution. To this solution, 12 ml of NH_4OH (25 wt %) dissolved in 48 ml distilled H_2O was added with stirring. The $SnCl_4$ solution (15 g of $SnCl_4$. $5H_2O$ dissolved in 150 ml distilled water) was added to the above solution (CTAB+ NH_4OH+H_2O) drop wise with continuous stirring to produce white slurry. The slurry was stirred for 3 h followed by ageing at room temperature for 48 h. The obtained product was filtered, washed with distilled water and dried at 120 ºC. Thus formed

white solid was calcined at different temperatures such as 300, 350, 400 and 500 ºC in the flow of air with heating rate of 2 ºC/min for 2 h.

The nano tin oxide was synthesized by the method as reported in the literature.[34] In a typical procedure, 11.3 g of $SnCl_4.5H_2O$ was dissolved in 25 ml of distilled water followed by addition of aqueous NaOH solution (7.5 g NaOH + 25 ml of H_2O). To the above solution, 2.5 g of CTAB was added with continuous stirring for 1 h. The precipitated solution was hydrothermally treated at 150 ºC for 4 h using teflon autoclave. The obtained precipitate was filtered, washed with distilled water and dried at 120 ºC. Thus formed white solid was calcined to 400 and 500 ºC. Bulk tin oxide was also prepared by the same procedure as given above without using the template. The tin oxide samples were designated as M-Y, where M is meso, nano or bulk type material and Y is the calcination temperature.

2.2. Catalyst characterization techniques

The phase purity and formation of meso, nano and bulk phase were determined by the X-ray diffractometer instrument (Bruker D-2 Phaser) with Cu K_α source (l -1.54 Å). The catalysts were analyzed in the 2 theta range of 1.5–60º with scanning rate of 1.2º/ min.

N_2 sorption measurements of all the tin oxide catalysts were carried out at -196 ºC in Quantachrome instrument. Prior to the analysis, the catalysts were heated to 150 ºC for 1 h. Specific surface areas of tin oxide catalysts were determined by Brunauer–Emmett–Teller (BET) equation. Average pore diameter and total pore volume of the catalysts were measured by BJH method. Scanning electron microscope (SEM) images of tin oxide catalysts were recorded in Zeiss microscope to investigate the particle size and morphology. The pore structure and crystal

types of the sample were analyzed by transmission electron microscope (TEM-JEOL-2010) with SAED.

The FT-IR (Bruker α-T model) spectra of the tin oxide catalysts were obtained in the range of 4000 to 500 cm^{-1}. To investigate the nature of acid sites present on the tin oxide, pyridine FT-IR technique was employed and spectra were recorded in the range of 1600–1400 cm^{-1}. The self-supported wafers of the catalysts were prepared by a pellet press instrument and the samples were saturated with pyridine followed by degassing at 150 ºC for 30 minutes as reported elsewhere. [29-31]

TGA curves were recorded simultaneously using a Universal V 2.4F-TA analyzer by heating the sample at the rate of 10 ˚C min^{-1} in flowing nitrogen gas. NH_3-TPD measurements were carried out by using the indigenous calibrated TPD instrument with TCD detector. In all the experiments, 200 mg of sample was calcined at respective temperature for 1 h in helium gas flow (25 mL min^{-1}) and then cool to 50 °C. At 50 °C, the sample was saturated with 10% of ammonia -helium stream for 1 h. After the saturation of ammonia, the sample was flushed with helium for 1 h at 50 °C to remove the physisorbed probe molecule. The desorption profile was performed in the temperature range from 50 to its respective temperature with a heating rate of 8 °C/ min.

2.3. Catalyst testing

All the reactions were carried out in liquid phase batch reactors at atmospheric pressure. In a typical procedure for Prins reaction, β-pinene (10 mmol), paraformaldehyde (20 mmol), catalyst (0.78 g) and solvent, benzonitrile (5 ml) were added to a 100 ml glass reactor equipped with a reflux condenser and a magnetic stirrer. The required temperature for the reaction was controlled and monitored by the PID temperature controller and thermometer respectively. After

the reaction, the product mixture was analyzed by gas chromatography (Shimadzu-2014, FID detector) using a RTX-5 column.

The glycerol carbonylation reaction was performed using glycerol (2 g), urea (1.3 g) and catalyst (0.66 g) in a 100 ml two necked glass reactor at 160 ºC. The N_2 gas was continuously purged through the second neck to remove ammonia formed during the reaction. After completion of the reaction, methanol was added to the reaction mixture and the catalyst was separated by centrifugation. The products were analyzed using gas chromatography by separating the products on 60 m X 0.25mm HP Innowax column. The products were confirmed by GCMS analysis. Similarly, glycerol ketalization and acetylation reactions were carried out in the absence of N_2 flow with the reaction conditions as shown in Table-4 and Table-5 respectively.

Catalyst recyclability study was carried out to check the efficiency of the catalyst. After the reaction, the catalyst was separated by filtration, washed with acetone and dried at 120 ºC for 12 h followed by activation at 300 ºC for 1 h. Thus obtained dried catalyst was reused for the next cycle.

3. Results and discussion

3.1. Characterization of catalysts

Fig.1. shows the low angle XRD pattern of the mesostructured tin oxide catalyst after calcination at different temperatures. The mesoporous tin oxide calcined at 300 ºC shows the presence of (100) diffraction peak due to the two-dimensional hexagonal structure. However, mesoporous tin oxide calcined above 350 ºC did not show any low angle diffraction peak which could be ascribed to the extensive sintering and collapse of the mesostructure at high temperatures.[35,36] The XRD patterns of the bulk and nano tin oxides exhibit a clear difference

between bulk and nano phase due to the variations in the broadness of the peaks that can be indexed to their corresponding crystalline tetragonal phase. The low intense broad diffraction peaks for the mesoporous tin oxide catalyst is due to the formation of nanocrystalline oxide domains.[32-36]

To find the particle size and morphology of bulk, nano and meso tin oxides, SEM images were collected as shown in Fig. 2. The mesoporous tin oxide showed non uniform particles with rough edge surfaces having particle size from 1 to 200 μm. The nano tin oxide exhibited spherical morphology with particle size in the nano range of 50-100 nm. The bulk tin oxide was found to show polygonal like morphology with average particle size of 1.5 μm. The SEM images further established the synthesized tin oxide catalysts are in the range of their bulk and nano scale.

To study the textural properties of the mesoporous tin oxide, N_2 sorption isotherms of catalysts calcined at different temperatures were measured. The surface area, pore volume and average pore diameter of tin oxide catalysts measured are tabulated in Table-1. The mesoporous tin oxide calcined at 300 ºC exhibited large surface area of 160 m^2/g. Further increase of calcination temperature to 350 and 500 ºC decreased the surface area to 105 and 51 m^2/g respectively. The surface area and total pore volume decreased with increase of calcination temperature which could be due to the sintering and destruction of pores at high temperature. [32,33] The calcined mesoporous tin oxide catalysts show distorted type IV isotherm with hysteresis loop in the P/Po region of 0.4 to 0.8. (Fig. S1) The Meso-300 and meso-350 showed H2-type hysteresis loop which could be due to the formation of spherical pores along with the cylindrical pores present in the materials and it also indicates the cavitation effect in ink-bottle type pores. However, H1-type hysteresis exhibited by meso-400 and meso-500 generally suggests a well-

defined cyclindrical-like pore channels present in the porous system.[37-39] The hysteresis loop broadens with increase of calcination temperature due to the formation of large pores at high temperatures.[36] This was further supported by measuring the pore size distribution of mesostructured tin oxide catalysts. (Fig. 3.) The average pore diameter increased from 34.5 to 67.9 Å with increase of catalyst calcination temperature from 300 to 500 ºC. On the contrary, the bulk and nano tin oxide showed lower surface area and pore volume compared to meso tin oxide.

Transmission electron microscopy (TEM) images of meso-300 show a wormhole like topology with no long range order as shown in Fig. 4. The selected area electron diffraction (SAED) pattern of meso-300 (Fig. 4.C) exhibited the concentric rings indicating the presence of very small crystallites with well-defined lattice planes (110), (101), (200) and (211). The meso-300 tin oxide showed well-defined lattice fringes with *d*-spacing of `~ 0.33 nm, corresponding to (110) plane of tetragonal rutile SnO_2 as shown in Fig. 4.d.[36] TEM image (Fig. 4.b) further confirmed the presence of nanocrystalline domains for meso-350 catalyst which is formed mainly due to the collapse of the mesopores wall. [36,40,41, 28.]

The TGA profile of mesoporous tin oxide exhibited weight loss in three steps as shown in Fig. S2. The as synthesized meso-120 catalyst showed initial weight loss below 110 ˚C due to desorption of water molecules. Second weight loss in the region of 120-400 ˚C is due to the removal of surfactant. The final small weight loss above 400 ˚C could be due to the removal residual surfactant and dehydroxylation. The mesoporous tin oxide catalyst calcined at different temperatures showed negligible weight loss compared to the as synthesized catalyst indicating complete removal of the surfactant. To further examine the efficiency of template removal, FT-IR spectra of CTAB and meso tin oxide catalyst were measured as shown in Fig. 5. The mesoporous tin oxide catalyst calcined at 300 and 400 ºC exhibited peaks at 3422 and 1626 cm^{-1}

due to the stretching and bending vibration of hydroxyl groups respectively, whereas peaks at 660 and 535 cm^{-1} are attributed to the Sn-O framework vibrations.[36] No peaks due to CH_2 (~2800 cm^{-1}) and C-C (~1500 and 900 cm^{-1}) bonds of CTAB were detected indicating a complete removal of template during calcination of meso SnO_2 catalyst.

To explore further on the acidity of catalysts, pyridine FT-IR spectra of the mesostructured tin oxide catalysts calcined at different temperatures were measured as shown in Fig. 6. The interaction of pyridine with the Brönsted and Lewis acid sites gives rise to bending vibrations at 1540 and 1450 cm^{-1} respectively. The respective, B/L values were determined by measuring the intensity of each peak as shown in Table-1. The mesostructured tin oxide showed the presence of both Brönsted and Lewis acid sites. The Brönsted acidity is due to the surface Sn-OH or hydrogen bonded Sn-OH groups, whereas Lewis acidity exists because of the framework Sn^{4+} sites. It is observed that increase of calcination temperature of mesoporous tin oxide catalyst decreased the intensity of the peak due to Brönsted acidity which could be attributed to the dehydroxylation of –OH group at higher temperatures. The B/L ratio of tin oxide catalysts decreases with increase of calcination temperature. These results clearly indicate that Meso-300 is highly Brönsted acidic in nature while meso-500 is Lewis acidic. The nano and bulk tin oxide showed less intense peak in py-FT-IR (not shown) indicating low acidic surface sites compared to mesoporous tin oxide.

To determine the amount and strength of acid sites temperature programmed desorption of ammonia (TPD-NH_3) was measured as shown in Fig. 7. The TPD-NH_3 measurements were carried out in the temperature range of 50-500 ˚C. TPD-NH_3 profiles of all the tin oxide catalysts exhibited a low temperature desorption peak at 150 ˚C which is due to the coordination of ammonia with weak acid sites. A peak was also observed above 400 ˚C in all the TPD profile.

However, similar kind of peak was also observed for tin oxide catalyst in absence of ammonia treatment and peak is considered to be due to the dehydroxylation of the surface –OH groups on the oxides and not due to the desorption of ammonia from acidic sites.(Fig. S4) Therefore, the total amount of acid sites was measured considering the only low temperature desorption peak as tabulated in Table-1. The total amount of acid sites decreased with increase of calcination temperature > 350 °C. The decrease of total acidity could be due to the decrease of surface area and dehydroxylation of surface active sites at higher temperature. The Meso-300 and Meso-350 showed almost similar acidity, whereas further increase of calcination temperature above 400 ˚C decreased acidity abruptly. The nano and bulk tin oxide catalyst showed lower acidity than the mesoporous tin oxide due to their lower surface area.

3.2. Catalytic activity studies

The efficiency of mesoporous tin oxide as a solid acid catalyst was established by accompanying four different acid catalyzed reactions involving conversion of biomass derived molecules through the activation of carbonyl group. One possible way to activate the carbonyl group is by polarization of the C=O bond, thereby generating electrophilic center. The polarization of the carbonyl group can be achieved by protonation (H^+) or interaction with Lewis acids typically by metal ions. Once the carbonyl group is polarized, it is easily get attacked by a nucleophile. (Scheme 1) Hence, the, activation of carbonyl group can be accomplished by using catalyst having Brönsted or Lewis acid sites.[42-44] The current organic transformations mainly proceed through the polarization of carbonyl group of an aldehyde, ketone, acetic anhydride or an amide.

3.2.1. Activation of an aldehyde

Activation of an aldehyde is a primary step in electrophillic addition of aldehyde to olefin over acidic catalysts known as Prins reaction.[29,45,46] Nopol produced by reacting activated formaldehyde with β-pinene is one of the industrially important chemicals used in perfumery, agrochemical and soap-detergent industries. Previous reports suggest that the aldehyde produced from paraformaldehyde in reaction media is activated by Lewis acid catalysts such as Sn-beta, Sn-MCM-41, Sn-SBA-15, Zr-SBA-15 and Zn-MCM-41, sulfated zirconia, mesoporous iron phosphate, Fe–Zn double cyanide complex, metal organic frameworks and Zn-Y.[29,47-55] Very few Brönsted acid catalysts such as Sn(OH)Cl and MWW type of zeolites were studied for this reaction.[46,56] The most of the above metal ion containing catalysts were synthesized by isomorphous substitution, wet impregnation, ion-exchange and chemical vapour deposition methods. These catalyst investigations indicate that weak Brönsted or strong Lewis acid sites are required for the selective synthesis of nopol.

The condensation of β-pinene with paraformaldehyde was carried out in liquid phase over the tin oxide catalysts and the results are as shown in Fig. 8. The as-synthesized mesoporous tin oxide showed lower conversion of 35 % with nopol selectivity of 92.3 %. As the calcination temperature of mesoporous tin oxide increased from 300 to 500 ºC, the conversion for β-pinene decreased from 82 to 50.4 %, whereas nopol selectivity increased from 85 to 98 % , respectively. The decrease of conversion could be due to decrease of active surface sites of the catalys upon calcination. The increase of nopol selectivity with increase of calcination temperature could be due to the decrease in Brönsted acid sites, because Brönsted acid sites are mainly responsible for the isomerization of β-pinene to side products like camphene, limonene and α-pinene. The nano

and bulk tin oxide catalysts showed lower β-pinene conversion (< 25 %) and nopol selectivity of ~50 % compared to the mesoporous tin oxide as shown in Fig. 8. The meso-350 showed high β-pinene conversion of 80 % with nopol selectivity of 93 %. The meso-350 catalyst was recycled thrice and exhibited excellent recyclability with negligible decrease in catalytic activity as shown in Table S3. These results clearly show that mesoporous tin oxide is potential solid acid catalyst in activation of the carbonyl group of aldehyde. The plausible reaction mechanism involving the activation of paraformaldehyde by tin oxide catalyst is shown in Scheme 2. Once the aldehyde molecule is adsorbed and coordinated to Sn acid sites (weak Brönsted and Lewis acid) the reaction is initiated by polarization of the C=O bond thereby generating an electrophilic centre which is then attacked by β-pinene to give an intermediate. Further allylic proton transfer forms a double bond resulting in to nopol. The β-pinene commonly undergoes isomerization over strong Brönsted acid catalyst to produce α-pinene, camphene and limonene. The high selectivity observed for nopol (> 85%) over mesoporous tin oxide catalyst clearly indicates the presence weak acid sites on the tin oxide catalyst.

Table 2. shows the comparison of catalytic activity of Meso-350 tin oxide with other reported solid acid catalysts. The Zr-SBA-15, Sn-kenyaite, Na-ITQ and Fe–Zn metal cyanide showed lower yield for nopol compared to meso-350. Zn-montmorillonite showed a slightly higher nopol yield (87%) compared to Meso-350 (present work). However, leaching of the Zn was observed during the reaction. The Prins reaction with sulphated zirconia Zn-beta was reported to give a high nopol yield. The tin based catalyst (SnSBA-5,Sn-MCM-41, Sn(OH)Cl showed higher activity and selectivity, however the catalyst were synthesized by tedious methods like chemical vapour deposition, maintaining the inert atmosphere and adjusting the proper pH for isomorphous substitution which makes challenging in large scale production for

industrial practice. The Meso-350 tin oxide catalyst with simple synthesis procedure, high catalytic activity and excellent recyclability is found to be a superior catalyst for practical commercial applications.

3.2.2. Activation of an amide

Glycerol carbonylation with urea to produce glycerol carbonate (GC) is one of the reactions which goes through activation of C=O group in urea.[30] The GC is synthesized by different routes such as reaction of glycerol with phosgene, carbonylation of glycerol with dimethyl carbonate or ethylene carbonate, carbonylation of glycerol by urea, reaction of glycerol with carbon dioxide. The main drawback of phosgene as carbonylating agent is its noxious nature. The use of carbon dioxide as carbonating agent needs high temperature and pressure results in too low yields for glycerol carbonate.[30] The use of ethylene carbonate as carbonylating agent is also attractive approach. However, the separation of formed GC from its by product (ethylene glycol) is difficult. The use of dimethyl carbonate as carbonate source requires basic catalyst. Nevertheless, these basic catalysts lose their activity after first use and easily get affected by moisture, making their practical applications difficult to practice.[30]

One of the adaptable routes for synthesis of glycerol carbonate from glycerol is the use of urea as carbonylating agent. The main benefit of this method is use of urea, which is an inexpensive readily available carbonate source and the by-product ammonia can be again utilized for the synthesis of urea, making it an atom efficient process. The glycerol carbonylation reactions are well-studied with Lewis acid catalysts such as ZnO, γ-zirconium phosphate, mixed metal oxides, HTc-Zn derived from hydrotalcite, Co_3O_4/ZnO, Sm and Zn exchanged heteropoly tungstate, Au supported ZSM-5, Zn-Y and $ZnSn(OH)_6$.[57-68] The glycerol carbonate product has a wide application as solvent, curing agent in cement, plasticizer, humectants, and nail lacquer gel

remover in the cosmetics industry, a liquid membrane in gas separation and an electrolyte in lithium-ion batteries.[69]

The catalytic activity of tin oxide catalysts for glycerol carbonylation reactions is tabulated in Table-3. The as-synthesized catalyst showed low glycerol conversion of 39 % with glycerol carbonate selectivity of 97 %. The glycerol conversion increased from 39 to 65 % with decrease in total acidity of meso tin oxide catalyst from 300 to 500 ºC. This could be due to the decrease of Brönsted acid sites in the catalyst, since Lewis acid sites are the major active sites for the reaction.[22] The selectivity for glycerol carbonate for all the catalysts was almost the same (97-99 %). The nano and bulk tin oxides showed lower glycerol conversion (37~42 %) compared to meso tin oxide due to the difference in morphology, structure and lower surface area. The meso-500 catalyst was recycled for three times with excellent recyclability as shown in Fig. S3. A plausible reaction pathway was given for glycerol carbonylation with urea to produce glycerol carbonate over tin oxide catalyst as shown in Scheme 3. It is speculated that Lewis acid sites activate (Sn^{4+}) the carbonyl group of the urea and weak conjugate base (framework oxygen) activates the hydroxyl group of the glycerol. Presence of these sites in meso tin oxide catalyst exhibited high catalytic activity and selectivity for glycerol carbonate in carbonylation reaction.

The activity of meso-500 catalyst was compared with other catalysts reported in the literature as shown in Table-3. The Sn-beta, Au/ Fe_2O_3 and Sm0.66 TPA showed good glycerol conversion with too low selectivity for glycerol carbonate. SW21 (Sn–W mixed oxide), 2.5% Au/Nb_2O_5 and Zn1TPA exhibited good selectivity for glycerol carbonate with low glycerol conversion. The zirconium phosphate exhibited high glycerol conversion (80%) and selectivity for glycerol carbonate (100%). The Meso-500 catalyst exhibited higher catalytic performance

than SW21, Sn-beta, Au/Fe_2O_3, $Sm_{0.66}$ TPA, 2.5% Au/Nb_2O_5 showing its prospective application as solid acid catalyst.

3.2.3. Activation of ketone

The ketalization of glycerol with cyclohexanone yields solketal, which in general precedes through the activation of carbonyl group of ketone.[31] The reactions of glycerol with cyclohexanone results in the formation of solketal which finds its application in cold flow improver to enhance cold weather performance of diesel fuel. Moreover, solketal blended with regular gasoline in different volume results in decrease of gum formation and enhances the octane number. The reaction is preferred the most over Brönsted acid catalysts such as SO_4^{2-}/TiO_2-La_2O_3, C/SO_3H and Sulfated Zirconia.[70-73]

The reaction of glycerol with cyclohexanone was carried out in liquid phase reactor at 40 ºC using tin oxide catalysts. The glycerol conversion and selectivity for 1,3-dioxolane (1, 4-dioxaspiro[4,5]decane-2-methanol) formed in the reaction are given in Table-4. The glycerol conversion decreased with increase of calcination temperature of meso tin oxide due to decrease in total acidity. The meso-300 showed 80.2 % glycerol conversation with 98 % 1,3-dioxolane selectivity, whereas for meso -500 conversion decreased to 60 % with 1,3-dioxalane selectivity of 90 %. Nevertheless, nano and bulk tin oxide exhibited lower conversion (~20-25 %). The recyclability study was carried out using the best catalyst, Meso-350 catalyst showing good recyclability with negligible (~ 3 %) decrease in the catalytic activity.(Table-4) These results suggest that the presence of Brönsted acidic sites on meso-tin oxide catalyst are adequate to activate the carbonyl group of ketone in glycerol ketalization reaction. The plausible reaction mechanism for ketalization reaction over tin oxide catalyst was as shown in Scheme S1. The comparison of the catalytic activity of meso tin oxide with other reported catalysts were also

illustrated in Table S2. The meso tin oxide showed higher catalytic activity compared to the, C-SO_3H, sulfated zirconia and $[Cp^*IrCl_2]_2$ catalysts. The SO_4^{2-}/TiO_2-La_2O_3 showed comparable ketal yield of (97 %) meso tin oxide catalyst. These results evidently indicate the application of meso tin oxide as a prospective acid catalyst for reaction involving activation of ketone.

3.2.3. Activation of acetic anhydride

Acetylation of glycerol with acetic anhydride produces mono, di and tri acetates. Glycerol acetins, namely di and triacetin, have major applications in cryogenics, plastics, and fuel additives. The acetylation of glycerol with acetic anhydride is preferred owing to its high selectivity for do and tri acetins than using acetic acid as acetylating agent.[74] The reaction is catalyzed by the activation of carbonyl group of acetic anhydride. Several, heterogeneous catalysts such as amberlyst-15, zeolite H-beta, montmorillonite K-10 and niobium phosphate are reported.[74] The reaction is mainly catalyzed by Brönsted acid sites and product selectivity mainly depends on the porous nature of the catalyst.

Table-5 shows the catalytic activity of meso-tin oxide catalyst towards glycerol acetylation of acetic anhydride in comparison with nano and bulk froms. All the meso tin oxide catalysts showed almost complete conversion with change in selectivity for acetins. Di and tri acetin selectivity decreased from meso-300 to meso-500, which could be due to the decrease of B/L ratio and increase of pore structure. Among the mesoporous tin oxides, meso-300 exhibited complete glycerol conversion of 100 with excellent di+triacetin selectivity (~93%). Nevertheless, nano and bulk tin oxides exhibited glycerol conversion of 80% with low selectivity for di and tri acetin (~30%). The best catalyst, Meso-350 was used for the recycle study and the catalyst showed a slight decrease in glycerol conversion (~6 %) after 3 recycles. The selectivity for di and tri acetin was also decreased with each recycle which could be due the blockage of some of

active sites due to adsorption of reactant on the catalyst. The plausible reaction mechanism for acetylation reaction over tin oxide catalyst was as shown in Scheme S2. To check the efficiency of the catalyst, meso- tin oxide catalyst was compared with other reported catalysts as shown in Table-5. The Meso-SnO_2 catalyst showed almost complete glycerol conversion at 40 ˚C compared to other reported catalysts which exhibited complete conversion at 60 ˚C. However the selectivity for tri acetin was low for Meso-SnO_2 compared to reported catalyst. The meso tin oxide catalyst showed high di-acetin selectivity showing its potential application as a solid acid catalyst.

The current results clearly indicate the potential application of mesoporous tin oxide as an acid catalyst in the activation of carbonyl group for certain organic transformations involving the conversion of biomass derived molecules. Investigations on the applications for several other acid catalyzed organic reactions and modifications to improve the catalyst properties are under development. The explorations of other mesoporous metal oxides such as ZrO_2, TiO_2, Fe_2O_3, Al_2O_3, Nb_2O_5 etc as solid acid catalysts are under investigation.

4. Conclusions

The present study describes the mesoporous tin oxide as a simple, efficient and eco-friendly solid acid catalyst for the activation of carbonyl group in selected organic transformations. The characterization of mesoporous tin oxide by XRD, N_2 sorption and TEM showed the retention of mesoporosity at lower calcination temperature of 300 ºC. Calcination of mesoporous tin oxide at high temperature resulted in destruction of pores and at the same time formation of nanocrystalline particles leading to lower surface area and pore volume. The FT-IR measurement showed the complete removal of the organic template (CTAB) at the calcinations temperature of 300 ºC. The py-FT-IR measurement showed the presence of both Brönsted and

Lewis acid sites on tin oxide due to the Sn-OH and framework Sn^{4+} sites respectively. The Brönsted acidity decreased with increase of calcination temperature due to the dehydroxylation of –OH groups. The mesoporous tin oxide showed higher catalytic performance in Prins reaction, glycerol acetylation, ketalization and carbonylation reactions compared to the nano and bulk tin oxide. The meso-350 gave high β-pinene conversion of 80 % with 93 % nopol selectivity. Meso -350 exhibited complete conversion of glycerol with high selectivity for di and tri acetins. Meso-500 showed glycerol conversion of 65 % with glycerol carbonate selectivity of 99 % which was considerably higher compared to the catalysts reported in the literature. The excellent catalytic performance of mesoporous tin oxides calcined at different temperatures are attributed to the presence of different nature of active sites and amount of acidity. All the catalyst showed excellent recyclability and good activity comparable to the literature reported catalysts. These results clearly indicate the potential application of simple mesoporous tin oxide materials as acid catalysts.

5. Acknowledgement

Vijaykumar S. M and P. Manjunathan acknowledge Admar Mutt Education Foundation (AMEF) for fellowship and facilities. Authors are thankful to CENSE, Indian Institute of Science, Bangalore for SEM analysis

6. References

[1] C. T. Kresge, M. E. Leonowicz, W. J. Roth, J. C. Vartuli, J. S. Beck, *Nature*., 1992, **359**, 710.

[2] J. S. Beck, J. C. Vartuli, W. J.Roth, M. E. Leonowicz, C. T. Kresge, K. D. Schmitt, C. T-W. Chu, D. H. Olson, E. W. Sheppard, S. B. McCullen, J. B. Higgins, J. L. Schlenker, *J. Am.*

Chem. Soc., 1992, **114**, 10834.

[3] Q. Huo, D. I. Margolese, U. Ciesla, P. Feng, T. E. Gier, P. Sieger, R. Leon, P. M. Petroff, F.Schuth, G. D. Stucky, *Nature,* 1994, **368**, 317.

[4] U. Ciesla, D. Demuth, R. Leon, P. Petroff, G. Stucky, K. Unger, F. Schuth , *J. Chem. Soc., Chem. Commun.,* 1994, 1387.

[5] D-H Choi, R. Ryoo*, J. Mater. Chem.*, 2010, **20**, 5544.

[6] W. Guo, F. Kleitz, K. Cho, R. Ryoo, *J. Mater. Chem.*, 2010, **20**, 8257.

[7] Q. Huo, D. I. Margolese, U. Ciesla, D. G. Demuth, P. Feng, T. E. Gier, P. Sieger, A. Firouzi, B. F. Chmelka, F. Schuth, G. D. Stucky, *Chem. Mater.,* 1994, **6**, 1176.

[8] S. A. Bagshaw, T. J. Pinnavaia, *Angew. Chem., Int. Ed. Engl.,* 1996, **35**, 1102.

[9] D. M. Antonelli, J. Y. Ying, *Angew. Chem., Int. Ed. Engl.,* 1995, **34**, 2014.

[10] D. M. Antonelli, J. Y. Ying, *Angew. Chem., Int. Ed. Engl.,* 1996, **35**, 426.

[11] G. Pacheco, E. Zhao, A. Garcia, A. Sklyarov, J. J. Fripiat, *Chem. Commun.,* 1997, 491.

[12] Y. Ren, Z. Ma, P. G. Bruce, *Chem. Soc. Rev.,* 2012, **41**, 4909.

[13] M. Antonietti, G.A. Ozin, *Chem. Eur. J.,* 2004, **10**, 28.

[14] F. Jiao, J. L. Bao, A. H. Hill, P. G. Bruce, *Angew. Chem., Int. Ed.,* 2008, **47**, 9711.

[15] Z. F. Bian, J. Zhu, J. Wen, F. L. Cao, Y. N. Huo, X. F. Qian, Y. Cao, M. Q. Shen, H. X. Li, Y. F. Lu, Angew. *Chem., Int. Ed.,* 2011, **50**, 1105.

[16] H. Kim, J. Cho, *J. Mater. Chem.,* 2008, **18**, 771.

[17] A. Khoda, S. S. Mohajerzadeh, Y. Mortazavi, A. M. Miri. *Sens Actuat B.*, 2001, **80**, 267.

[18] Y. Idota, T. Kubota, A. Matsufuji, Y. Maekawa, T. Miyasaka. *Science.,* 1997, **276**, 1395.

[19] P. G. Harrison, C. Bailey, W. Azelee. *J Catal.*, 1999, **186**, 147.

[20] M. Caldararu, M. F. Thomas, J. Bland, D. Spranceana, *Appl Catal A.*, 2001, **209**, 383.

[21] B. Vishwanathan, "Catalysis Selected Applications" Chapter-4.3, ISBN: 978-81-7319-758-1, Narosa Publishing, India.

[22] A. Corma, S. Iborra, A. Velty, Chem. Rev., 2007, **107,** 2411.

[23] Y. L. Gu, A. Azzouzi, Y. Pouilloux, F. Jerome, J. Barrault, *Green Chem*., 2008, **10**, 164.

[24] M. Pagliaro, R. Ciriminna, H. Kimura, M. Rossi, C. D. Pina, *Angew. Chem., Int. Ed.,* 2007, **46**, 4434.

[25] C. H. Zhou, J. N. Beltramini, Y. X. Fan, G. Q. Lu, *Chem.Soc. Rev.,* 2008, **37**, 527.

[26] A. Behr, J. Eilting, K. Irrawaddy, J. Leschinski, F. Lindner, *Green Chem*., 2008, 10, 13.

[27] V. V. Costa, H. Bayahia, E. F. Kozhevnikova, E. V. Gusevskaya, I. V. Kozhevnikov, *ChemCatChem*, 2014, **6**, 2134.

[28] A. V. Subrahmanyam, S. Thayumanavan, G. W. Huber, *ChemSusChem*, 2010, 3, 1158.

[29] V. S. Marakatti, A. B. Halgeri, G. V. Shanbhag, *Catal. Sci.Technol.,* 2014, **4**, 4065.

[30] V. S. Marakatti, A. B. Halgeri, *RSC Adv*., 2015, **5**, 14286.

[31] P. Manjunathan, S. P. Maradur, A. B. Halgeri, G. V. Shanbhag, *J. Mol. Cat A: Chem.* 2015, **396**, 47.

[32] Y-D Wang, C. L. Ma, X. D Sun, H.D Li, Micro. Mesopor., 2001, **49,** 171.

[33] Y-D. Wang, C. L. Ma, X. D. Sun, H. D. Li, *Inorg. Chem. Commun.,* 2001, **4**, 223.

[34] J. Gajendiran, V. Rajendran, *Int. J. Mater, Biomater. Appl.,* 2012, **2**, 37.

[35] K. G. Severin, T. M. Abdel-Fattah, T. J. Pinnavaia, *Chem. Commun.,* 1998, 1471.

[36] J. Haiyan, D. Hongxing, X. Yunsheng, H. Hong, *Chin. J. Catal.,* 2010, **31**, 295.

[37] P. Sudarsanam, P. R. Selvakannan, S. K. Soni, S. K. Bhargava and B. M. Reddy, *RSC Adv.,* 2014, **4**, 43460.

[38] B. Malleshama, P. Sudarsanam, B. V. S. Reddy, B. M. Reddy, *Appl. Catal. B: Environ.,* 2016, **181**, 47.

[39] B. Mallesham, P. Sudarsanam, .G. Raju, B.M. Reddy, *Green Chem.,* 2013, **15**, 478.

[40] L. Qi, J. Ma, H. Cheng, Z. Zhao, *Langmuir.,* 1998, **14**, 2579.

[41] F. Chen, M. Liu, *Chem. Commun.*, 1999, 1829.

[42]A. Dhakshinamoorthy, M. Opanasenko, J. Cejka, H. Garciaa, *Adv. Synth. Catal.,* 2013, **355**, 247.

[43] S. V. Jadhav, K.M, Jinka, H. C. Bajaj, *Catal. Today.* 2012, **198**, 98.

[44] S. Shambayati, S. L. Schreiber, *Lewis Acid Carbonyl Complexation*, in *Comprehensive Organic Synthesis*, Trost, B.M.; Fleming, I., Eds. Pergamon, Oxford, 1991, vol. 1, chap. 1.10, pp. 283.

[45] V. S. Marakatti, G. V. Shanbhag, A. B. Halgeri, *Appl. Catal., A,* 2013, **451**. 71.

[46] V. S. Marakatti, G. V. Shanbhag, A. B. Halgeri, *RSC Adv.,* 2013, **3**, 10795.

[47] A. Corma, S. Iborra, M. Mifsud, M. Renz, *Arkivoc,* 2005, **9**, 124.

[48] E. A. Alarcón, L. Correa, C. Montes, A. L. Villa, *Micropor. Mesopor. Mater.* 2010, **136**, 59.

[49] M. Selvaraj, Y. Choe, *Appl. Catal., A,* 2010, **373**, 186.

[50] D. M. Do, S. Jaenicke, G. Chuah, *Catal. Sci. Technol*., 2012, **2**, 1417.

[51] E. A. Alarcón, A. L. Villa, C. M. Correa, *Micropor. Mesopor. Mater.*, 2009, **122**, 208.

[52] S. V. Jadhav, K. M. Jinka, H. C. Bajaj, *Appl. Catal., A*, 2010, **390**, 158.

[53] M. V. Patil, M. K. Yadav, R. V. Jasra, *J. Mol. Catal. A: Chem.,* 2007, **273**, 39.

[54] U. R. Pillai, E. S. Demessie, *Chem. Commun.,* 2004, 826.

[55]M. Opanasenko, A. Dhakshinamoorthy, Y. Hwang, J. Chang, H. Garcia, J. Čejka, *ChemSusChem.*, 2013, **6**, 865.

[56] J. Wang, S. Jaenicke, G. K. Chuah, W. Hua, Z. Gao, *Catal. Commun*., 2011, **12**, 1131

[57] F. Rubio-Marcos, V. Calvino-Casilda, M. A. Ba˜nares, J. F. Fernandez, *J. Catal.,* 2010, **275**, 288.

[58] C. Hammond, J. A. Lopez-Sanchez, M. H. Ab Rahim, N. Dimitratos, R. L. Jenkins, A. F. Carley, Q. He, C. J. Kiely, D. W. Knight, G. J. Hutchings, *Dalton Trans.,* 2011, **40**, 3927.

[59] L. Wang, Y. Ma, Y. Wang, S. Liu, Y. Deng, *Catal. Commun.,* 2011, **12**, 1458.

[60] Y. T. Algou, B. H. Hameed, *Fuel Process. Technol.,* 2014, **126**, 5.

[61] J. W. Yoo, Z. Mouloungui, *Stud. Surf. Sci. Catal.,* 2003, **146**, 757.

[62] M. Aresta, A. Dibenedetto, F. Nocito, C. Ferragina, *J. Catal.,* 2009, **268**, 106.

[63] K. Jagadeeswaraiah, C. Ramesh Kumar, P. S. Sai Prasad, S. Loridant, N. Lingaiah, *Appl. Catal., A,* 2014, **469**, 165.

[64] M. J. Climent, A. Corma, P. Frutos, S. Iborra, M. Noy, A. Velty, P. Concepcion, *J. Catal.,* 2010, **269**, 140.

[65] F. Rubio-Marcos, V. Calvino-Casilda, M. A. Ba˜nares, J. F. Fernandez, *J. Catal.,* 2010, **275**, 288.

[66] C. Ramesh Kumar, K. Jagadeeswaraiah, P. S. Sai Prasad, N. Lingaiah, *ChemCatChem.,* 2012, **4**, 1360.

[67] K. Jagadeeswaraiah, C. Ramesh Kumar, P. S. Sai Prasad, N. Lingaiah, *Catal. Sci.Technol.,* 2014, **4**, 2969.

[68] S. Swetha, G. V. Shanbhag, A. B. Halgeri, *RSC Adv*., 2014, **4**, 974.

[69] M. O. Sonnati, S. Amigoni, E. Givenchy, T. Darmanin, O. C. F. Guittard, *Green Chem*., 2013, **15**, 283.

[70] C. Crotti, E. Farnetti, N. Guidolin, *Green Chem.*, 2010, 12, 2225.

[71] S. Qianqian, L. Qun; X. Guomin, *Dongnan Daxue Xuebao, Ziran Kexueban* 2011, 41, 140.

[72] G. Wenyi; Z. Xiaoli; R. Liguo, *Xiangliao Xiangjing Huazhuangpin* 2011, 28, 17.

[73] O. Elena-Emilia; S. Emil; R. Paul; R. Adrian; E. Cristina-Emanuela. *Analele Universitatii "Ovidius" Constanta, Seria: Chimie, 2012, 23*, 72

[74] L. N. Silva, Va L.C. Gonçalves, C. J.A. Mota, *Catal. Commun*. 2010, 11, 1036.

[75] M. K. Yadav, R. V. Jasra, *Catal. Commun*., 2006, 7, 889.

[76] M. Aresta, A. Dibenedetto, F. Nocito, C. Pastore, *J. Mol. Catal. A: Chem.,* 2006, **257**, 149.

[77] C. Aille, J. W. Yoo, S. Pelet, Z. Mouloungui, *Catal. Lett.,* 1998, **56**, 245.

[78] C. Hammond, J.A. Lopez-Sanchez, M. H. Ab Rahim, N. Dimitratos, R. L. Jenkins, A. F. Carley, Q. He, C. J. Kiely, D.W. Knight, G. J. Hutchings, *Dalton Trans.,* 2011, 40, 3927

Figure Legends

Fig. 1. The low angle XRD patterns of mesostructured tin oxides calcined at different temperatures and wide angle XRD patterns of meso, nano and bulk tin oxide calcined at 400 ºC.

Fig. 2. SEM image of a)nano b)bulk and C) meso tin oxide catalysts.

Fig. 3. BJH Pore size distribution plot for calcined mesostructured SnO_2 (a) 300 ºC (b) 350 ºC (c) 400 ºC (d) 500 ºC

Fig. 4. TEM images of Meso-300 (a, c and d) and Meso-350 (b).

Fig. 5. FT-IR spectra of CTAB, meso-300 and meso -400 tin oxide catalysts.

Fig. 6. The py-FTIR acidity measurement of mesostructured tin oxide calcined at different temperatures.

Fig. 7. TPD-NH_3 profile of mesoporous tin oxide catalysts.

Fig. 8. Catalytic performance of tin oxide catalysts in activation of aldehyde for Prins condensation reaction.

Reaction conditions: ß-pinene = 1.36 g, Paraformaldehyde =0.6 g, Benzonitrile = 5 ml, catalyst amount = 0.78 g, reaction temperature = 90 ºC, reaction time = 10 h.

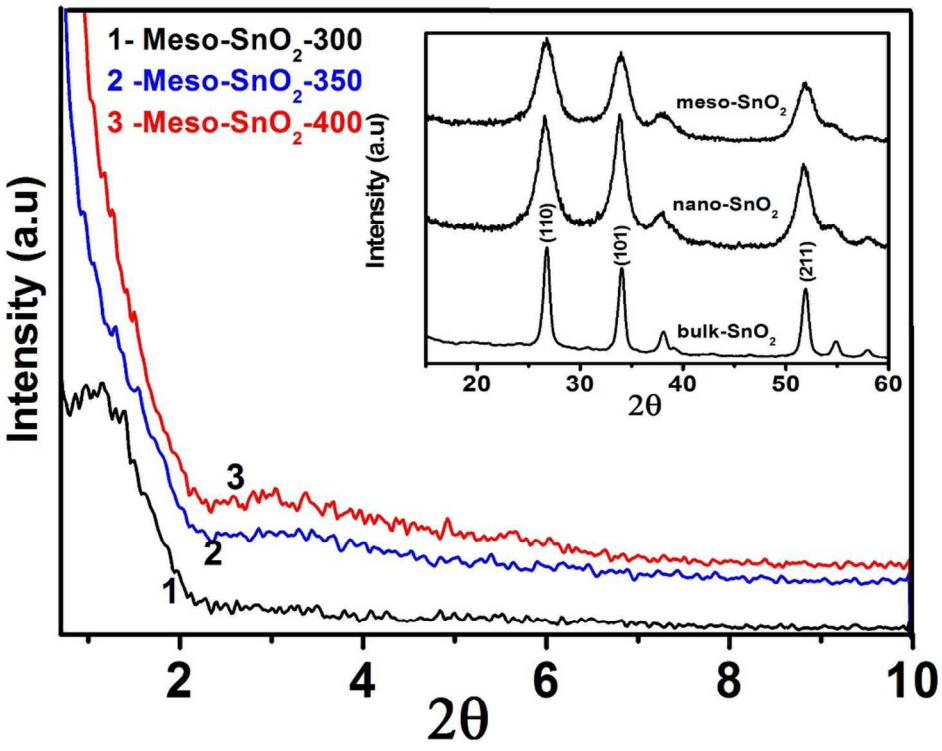

Fig. 1.

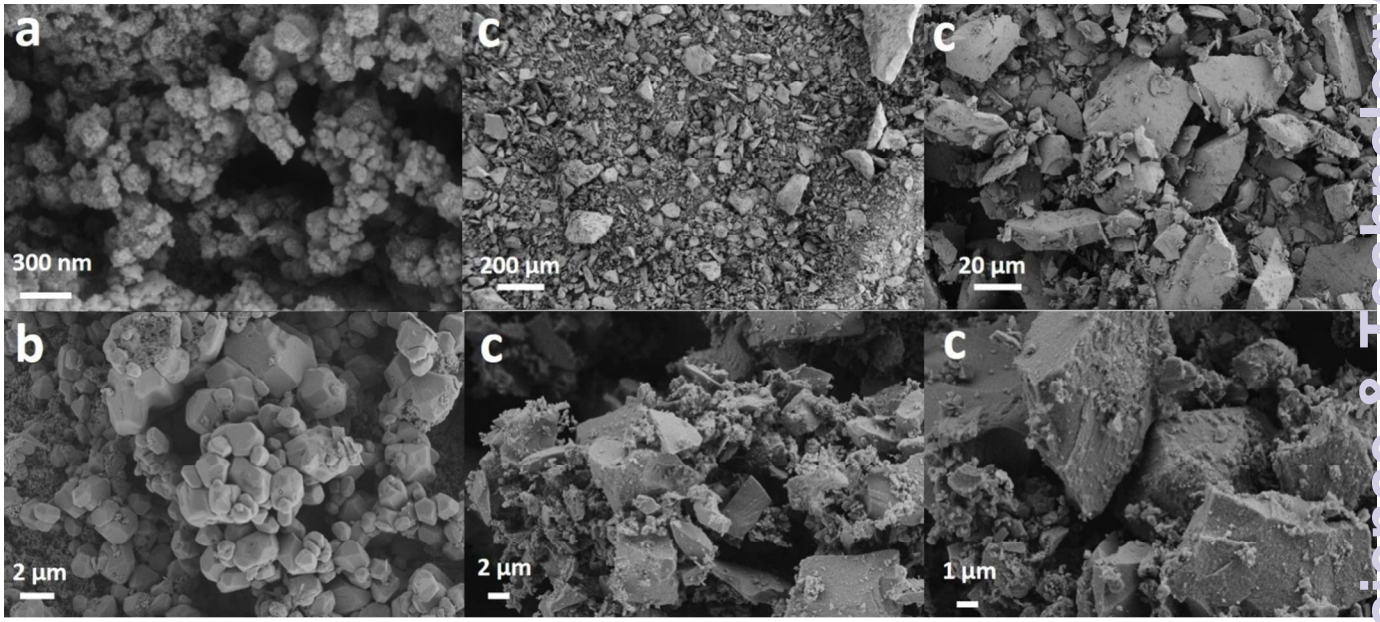

Fig. 2.

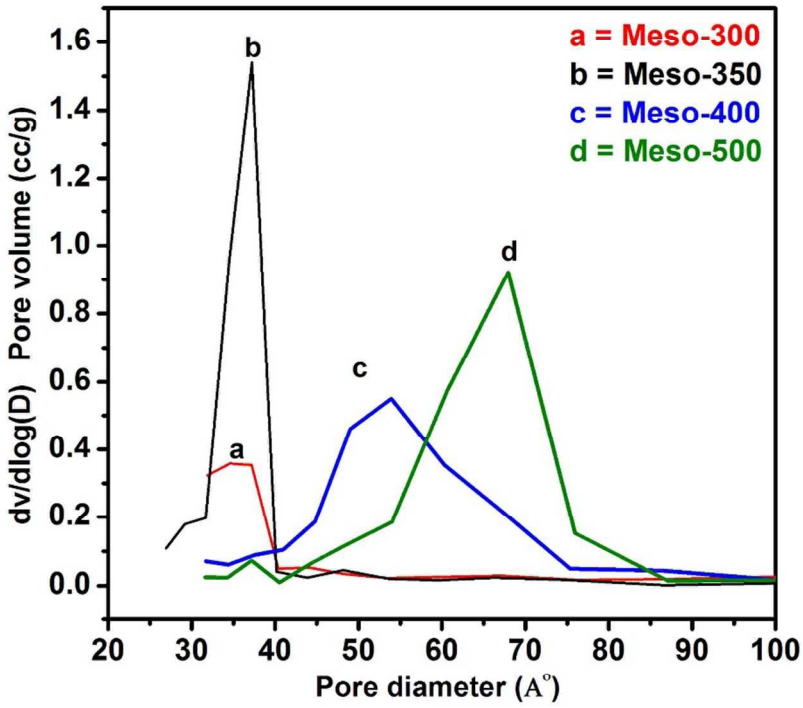

Fig. 3

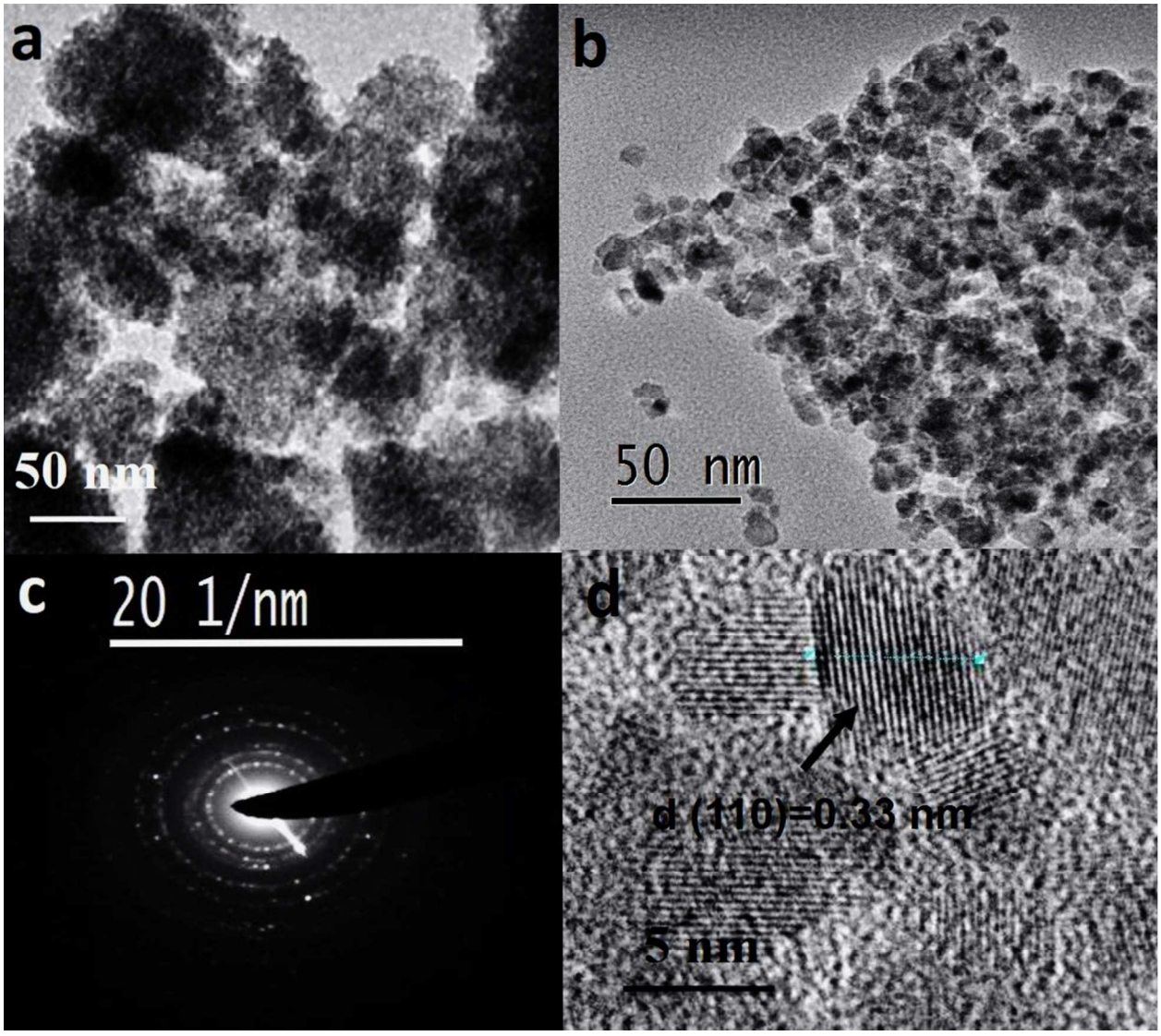

Fig. 4.

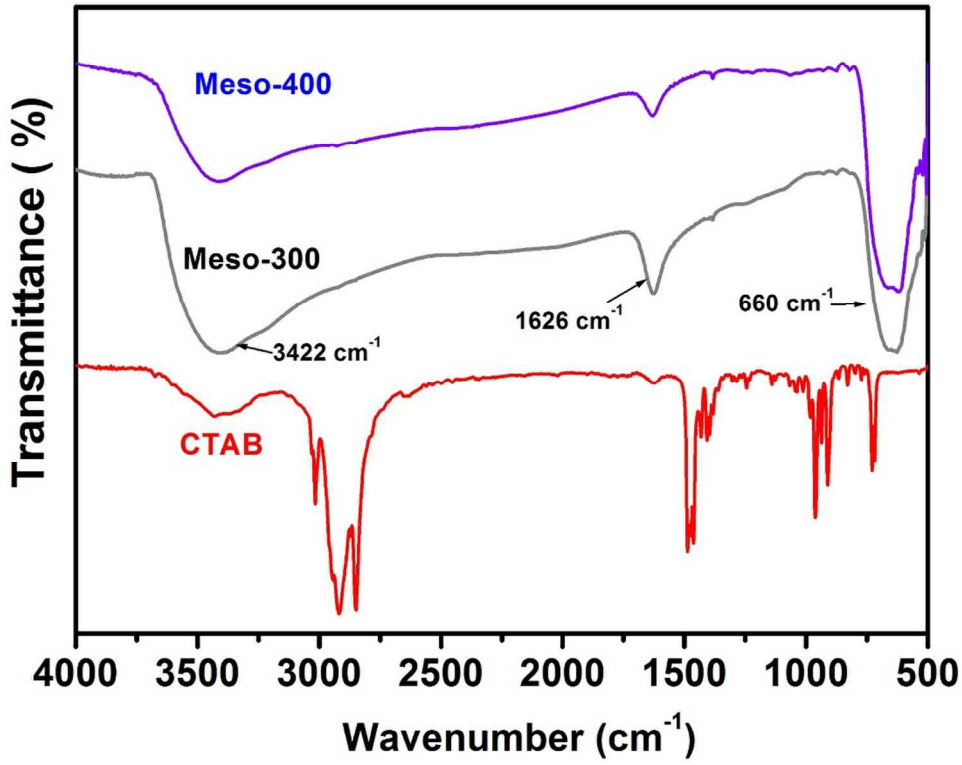

Fig. 5.

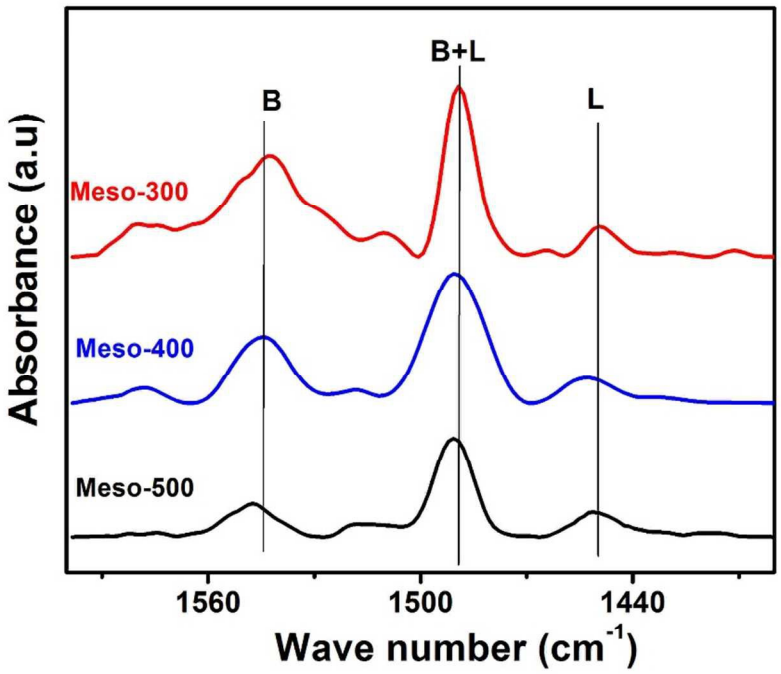

Fig. 6.

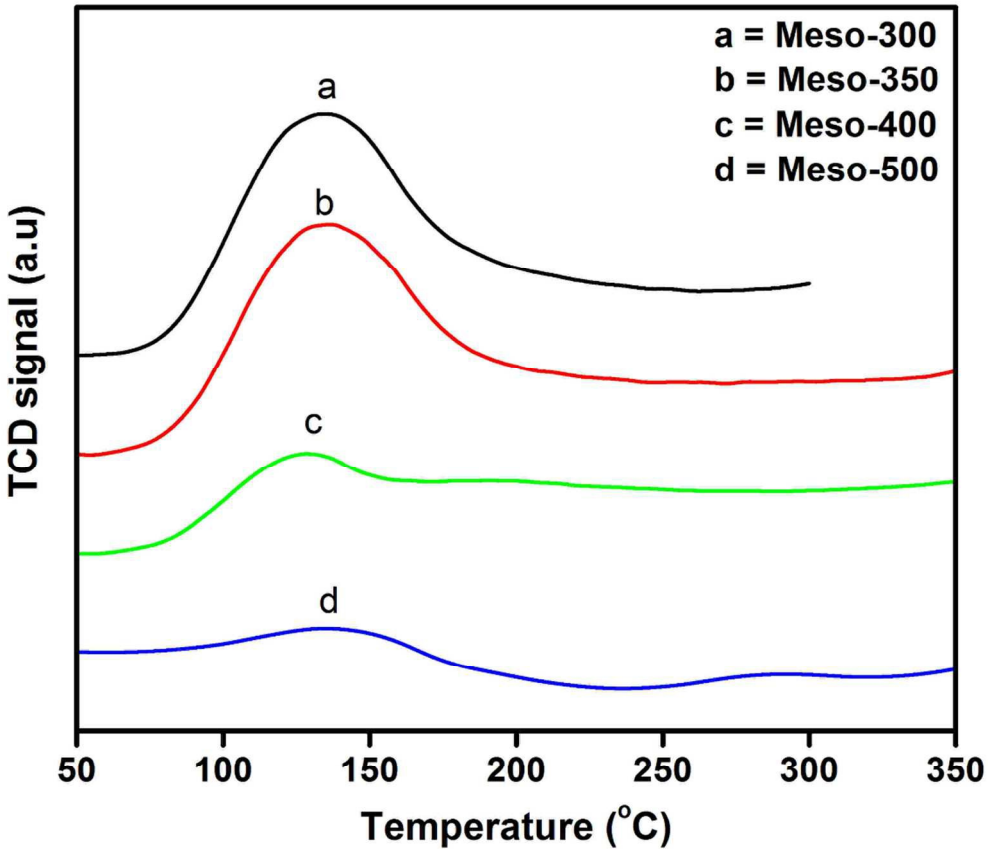

Fig. 7.

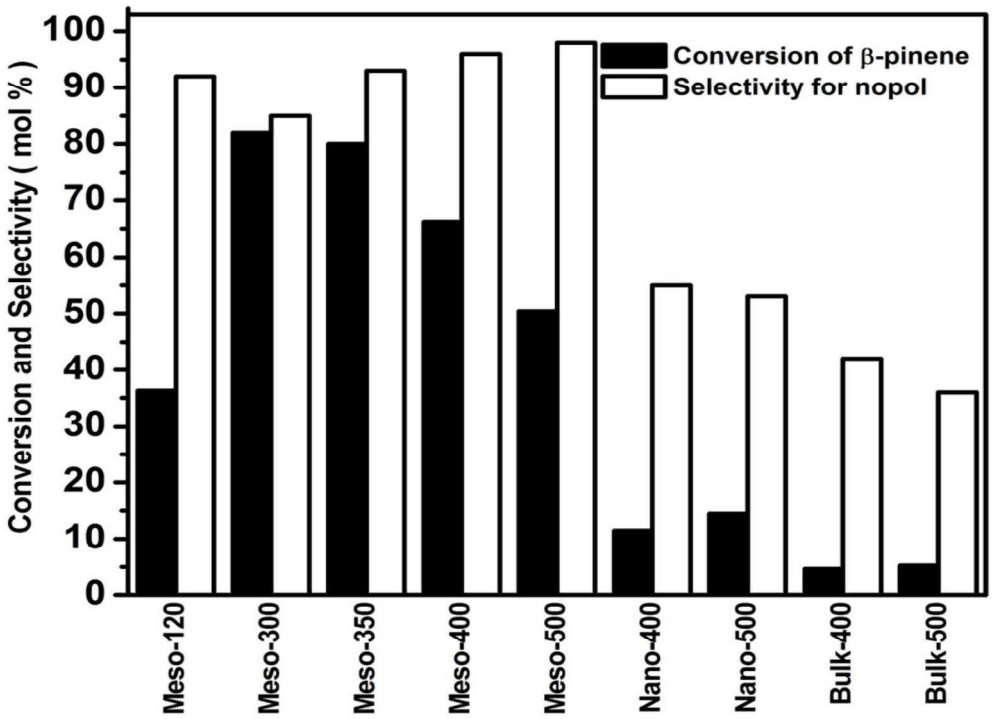

Fig. 8.

Table Legends

Table-1 Structural and acidic properties of tin oxide catalysts.

Table-2 Comparison of catalytic activity of the meso-SnO_2 catalyst with other reported solid acid catalyst.

Table-3 Catalytic activity of tin oxides and other reported catalyst in glycerol carbonylation reaction with urea to glycerol carbonate.

Table-4 Ketalization of glycerol with cyclohexanone over tin oxide and other reported catalysts.

Table-5 Catalytic activity of tin oxide and other reported catalysts towards acetylation of glycerol with acetic anhydride.

Table-1 Structural and acidic properties of tin oxide catalysts.

Catalyst	Surface area (m^2/g)	Pore volume (cc/g)	Average Pore diameter (Å)	Acidity measurement	
				Pyridine – FT-IR (B/L)	TPD-NH_3 (mmol NH_3/g)
Meso-300	160	0.121	34.5	3.5	0.44
Meso-350	105	0.110	37.2	3.2	0.41
Meso-400	55	0.103	53.9	2.5	0.29
Meso-500	51	0.099	67.9	1.4	0.24
Bulk-500	35	0.061	37.3	--	0.11
Nano-500	43	0.079	67.6	--	0.24

Table 2 Comparison of catalytic activity of the meso-SnO_2 catalyst with other reported solid acid catalyst

Catalyst	**β-pinene Conversion (%)**	**Nopol Yield (%)**	**Refrences**
Sn-SBA-15	99.8	98.7	49
Sn-MCM-41	99.3	98	48
Sn-Kenyaite	50.8	49.8	48
Sn(OH)Cl	98	97	46
Sulfated Zirconia	99	98	52
Na-ITQ	60	52.2	56
Zr-SBA-15	74	74	50
Zn-Montmorillonite	90	87.3	75
Fe-Zn metal cyanide	52	49.9	53
Zn-MCM-41	91	75.5	48
Zn-beta	92	85.5	29
Meso-350	80	74.4	**Present work**

Table-3 Catalytic activity of tin oxides and other reported catalyst in glycerol carbonylation reaction with urea to glycerol carbonate.

Catalysts	Glycerol conversion (mol %)	Glycerol carbonate selectivity (mol %)	References
Meso -120	39	97	--
Meso -300	45	99	--
Meso -350	50	99	--
Meso -400	54	100	--
Meso -500	65	98	--
Nano-500	37	98	--
Bulk-500	42	100	--
SW21	52.1	95.3	61
Sn-beta	70	37	76
Zr-P	80	100	77
Au/Fe2O3	80	48	78
Zn-Y	94.6	98	30
2.5% Au/Nb_2O_5	49.5	85.4	78
Zn_1TPA	69.2	99.4	66

Reaction conditions: glycerol = 2 g, urea =1.30 g, catalyst amount = 0.66 g, reaction temperature = 160 ºC, reaction time 4 h.

Table-4 Ketalization of glycerol with cyclohexanone over tin oxide and other reported catalysts.

Catalyst	Glycerol conversion (mol %)	Selectivity for ketal (mol %)	Yield for ketal	References
Blank	4.0	93	3.7	-
Meso-300	80.2	98	78.5	-
Meso-350	79.8	98	78.2	-
Meso-400	70.6	96	67.7	-
Meso-500	60.0	94	56.4	-
Nano-500	25.0	94	23.5	-
Bulk-500	20.0	95	19.0	-
Meso-350 R-1[a]	78.5	98	-	-
Meso-350 R-2[a]	77.0	98	-	-
Meso-350 R-3[a]	75.2	98	-	-
$[Cp^*IrCl_2]_2$	-	-	73.7	70
SO_4^{2-}/TiO_2-La_2O_3	-	-	97.0	71
C/SO_3H	-	-	92.0	72
Sulfated Zirconia	-	-	85.0	73
Meso-350*	94	99	93.0	Present work

Reaction conditions: Glycerol = 10 mmol, Cyclohexanone = 10 mmol, catalyst amount = 5 wt% (referred to glycerol weight), temperature = 40 ºC, reaction time = 1 h [a] Recycle studies.* Reaction carried out at 100 ˚C.

Table-5 Catalytic activity of tin oxide and other reported catalysts towards acetylation of glycerol with acetic anhydride.

Catalyst	Glycerol conversion (mol %)	Selectivity for acetins (mol %)			Di + Tri acetin selectivity (mol %)
		Mono	Di	Tri	
Blank	48.7	90.1	9.7	0.2	9.9
Meso-300	100	7.0	58.0	35.0	93.0
Meso-350	100	9.1	60.9	30.0	90.9
Meso-400	100	26.0	60.0	14.0	74.0
Meso-500	97.3	36.7	54.2	9.1	63.3
Nano-500	81.8	68.9	30	1.1	31.1
Bulk-500	83.3	64.4	34.1	1.5	35.6
Meso -350 R-1[a]	96.4	35.6	54.5	9.9	64.4
Meso -350 R-2[a]	95.0	41.5	50.9	7.6	58.5
Meso -350 R-3[a]	94.0	46.9	47.1	6.0	53.1
[b]H-beta	100	--	38	62	100
[b]K-10	100	--	22	78	100
[b]Amberlyst-15	100	--	10	90	100
[b]Niobium Phosphate	100	--	53	47	100
Meso-500[c]	100	3	56.5	40.5	97

Reaction condition: Glycerol = 0.92 g, Acetic anhydride = 4.08 g, catalyst amount = 0.20 g, temperature = 40 ^{o}C, reaction time = 2 h, [a] R = Recycle studies. [b] From reference [71]. [c] Reaction carried out at 60 ˚C.

Scheme 1. Activation of carbonyl group by mesoporous tin oxide catalysts.

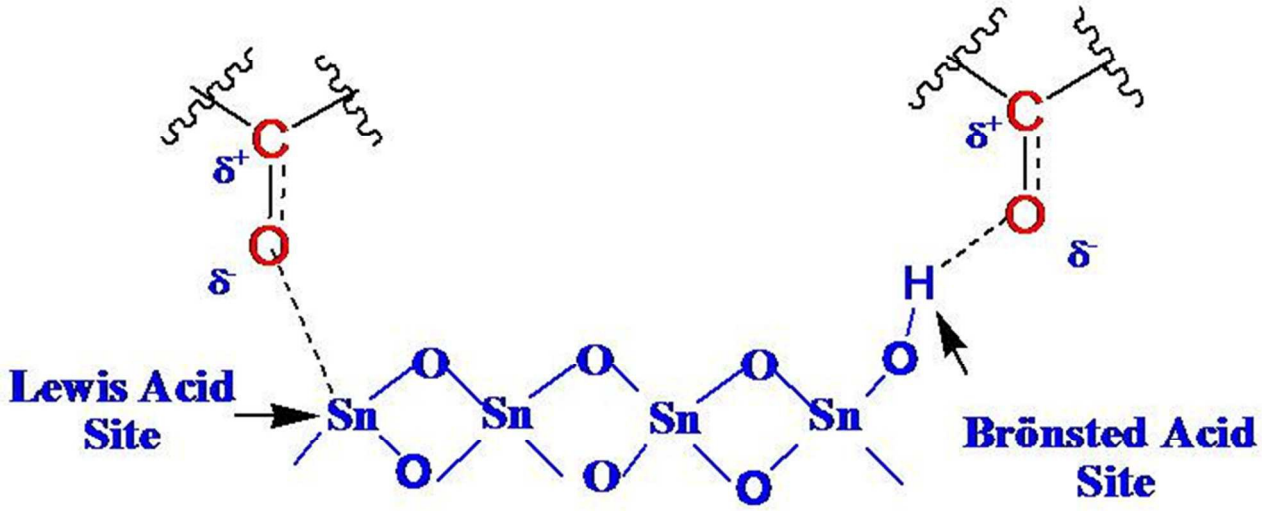

Scheme 2. The plausible reaction mechanism of Prins reaction over meso-SnO_2 catalyst

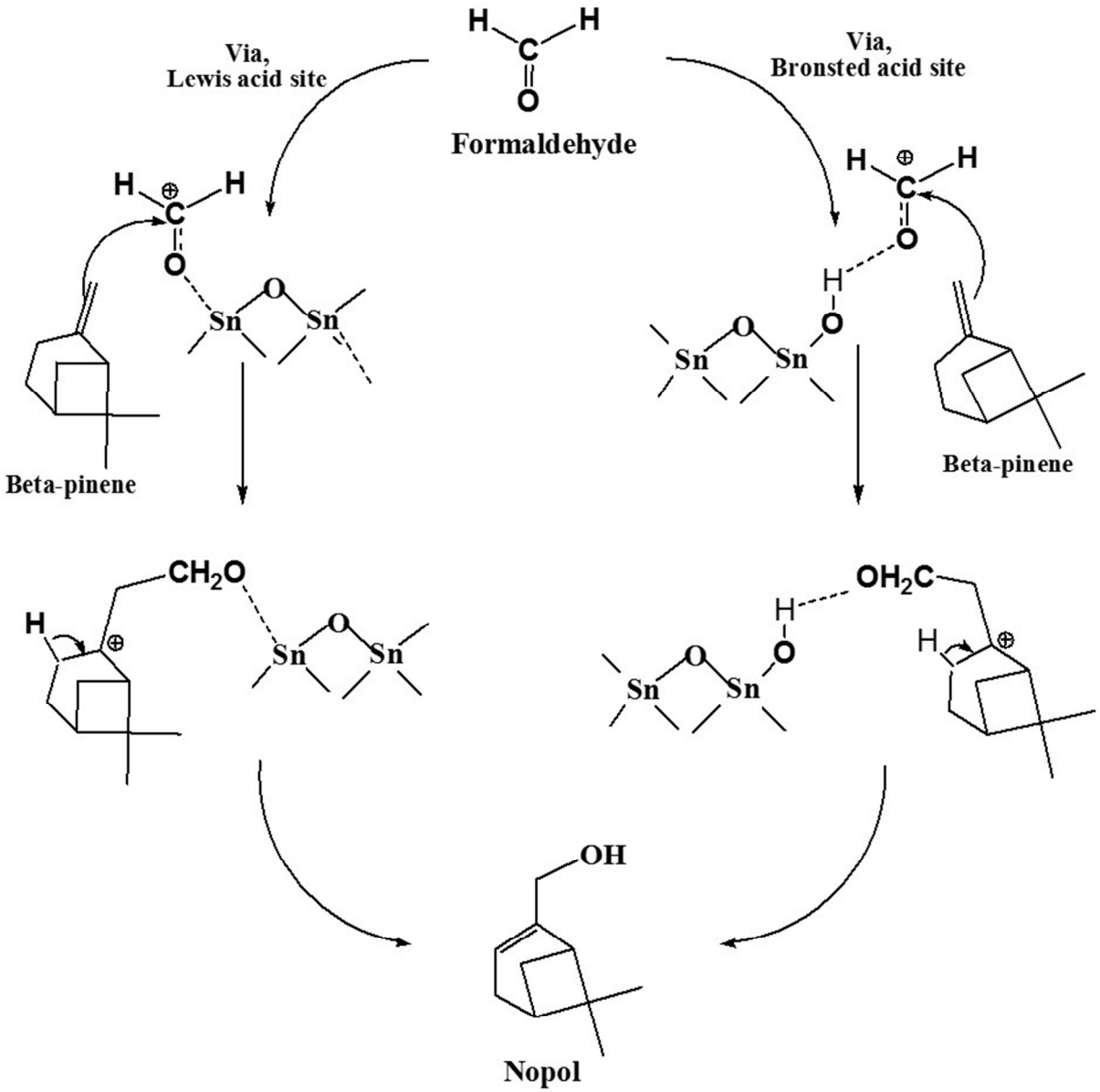

Scheme 3. The plausible reaction pathway for glycerol carbonylation with urea to produce glycerol carbonate over tin oxide catalyst.

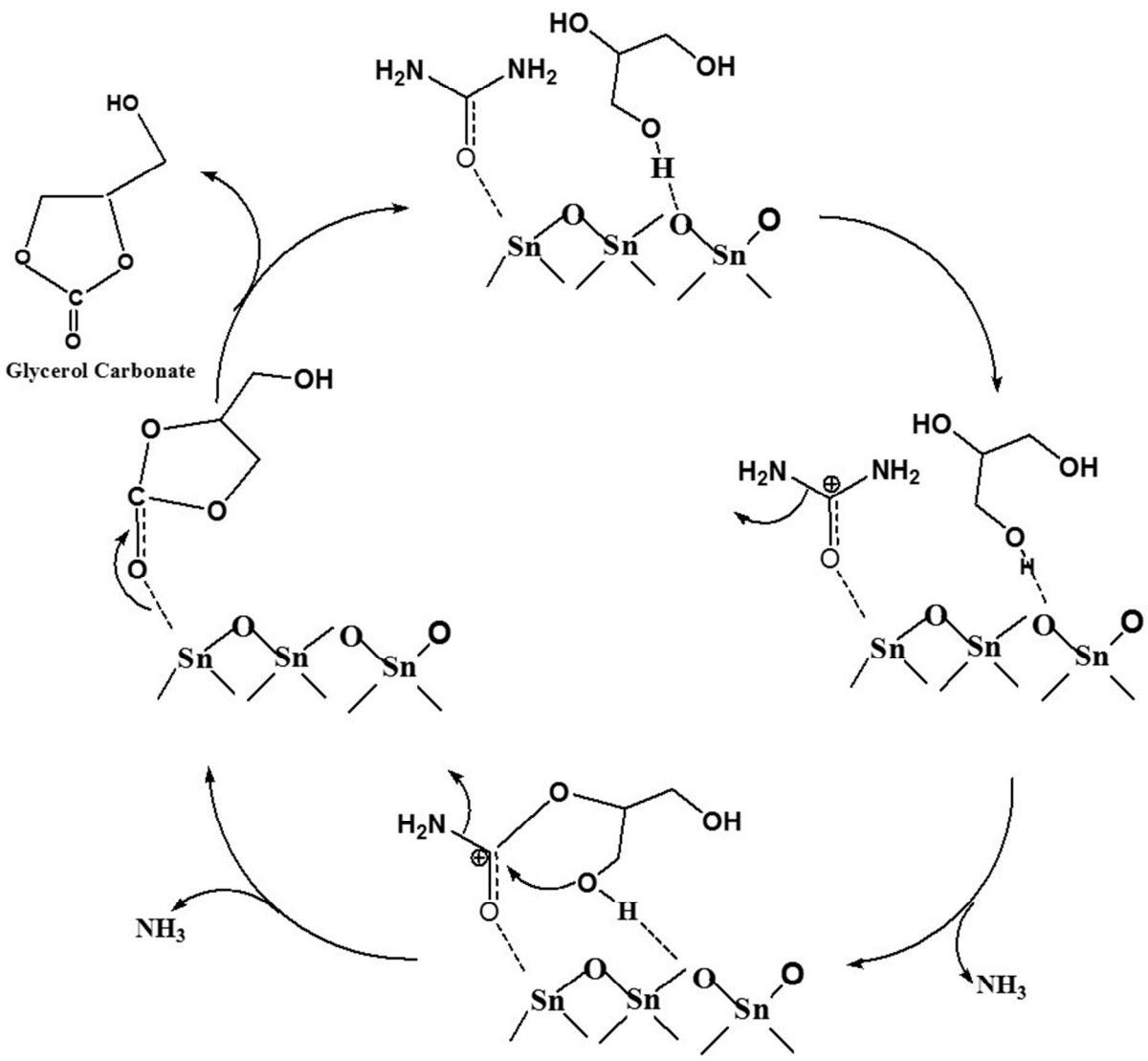

Graphical abstract: